Bone 121 (2019) 212–220

Contents lists available at ScienceDirect

Bone

journal homepage: www.elsevier.com/locate/bone

Full Length Article

Clinical and genetic analysis in a large Chinese cohort of patients with X-linked hypophosphatemia

Cong Zhang[a], Zhen Zhao[a,b], Yue Sun[a], Lijun Xu[a], Ruizhi JiaJue[a], Lijia Cui[a], Qianqian Pang[a], Yan Jiang[a], Mei Li[a], Ou Wang[a], Xiaodong He[a,c], Shuli He[a], Min Nie[a], Xiaoping Xing[a], Xunwu Meng[a], Xueying Zhou[a], Lina Yan[d], Jared M. Kaplan[e], Karl L. Insogna[e], Weibo Xia[a,*]

[a] Department of Endocrinology, Key Laboratory of Endocrinology, Ministry of Health, Peking Union Medical College Hospital, Chinese Academy of Medical Sciences & Peking Union Medical College, Shuaifuyuan No. 1, Wangfujing, Dongcheng District, Beijing 100730, China
[b] Department of Geriatrics, Beijing Friendship Hospital Affiliated to Capital Medical University, Beijing 100050, China
[c] Department of Endocrinology, The First Affiliated Hospital of Xinjiang Medical University, Urumqi 830054, China
[d] Department of Endocrinology, Baogang Hospital, Baotou, Inner Mongolia 014000, China
[e] Department of Medicine, Section of Endocrinology, Yale School of Medicine, New Haven, CT, USA

ARTICLE INFO

Keywords:
X-linked hypophosphatemia (XLH)
PHEX
Genetic analysis
Sex difference
Genotype-phenotype correlation
3D model of PHEX

ABSTRACT

X-linked Hypophosphatemia (XLH) is caused by loss of function mutations in the *PHEX* gene. Given the recent availability of a new therapy for XLH, a retrospective analysis of the most recent 261 Chinese patients with XLH evaluated at Peking Union Medical College Hospital was conducted. Clinical, biochemical, radiographic studies, as well as genetic analyses, including Sanger sequencing for point mutations and Multiplex Ligation-dependent Probe Amplification (MLPA) to detect large deletions/duplications were employed. Based on the structure of Neprilysin (NEP), a member of M13 family that includes PHEX, a three-dimensional (3D) model of PHEX was constructed, missense and nonsense mutations were positioned on the predicted structure to visualize relative positions of these two types of variants. Sex differences and genotype-phenotype correlations were also undertaken.

Genetic analyses identified 166 *PHEX* mutations in 261 XLH patients. One hundred and eleven of the 166 mutations were unreported. Four mutational 'hot-spots' were identified in this cohort (P534L, G579R, R747X, c.1645+1 G > A). Missense mutations, but not nonsense mutations, clustered in the two putative lobes of the PHEX protein, suggesting these are functionally important regions of the molecule. Circulating levels of intact FGF23 were significantly elevated (median level 101.9 pg/mL; reference range 16.1–42.2 pg/mL). No significant sex differences, as well as no phenotypic differences were identified between patients with putative truncating and non-truncating *PHEX* mutations. However, patients with N-terminal *PHEX* mutations had an earlier age of onset of disease (P = 0.015) and higher iFGF23 levels (P = 0.045) as compared to those with C-terminal mutations.

These data provide a comprehensive characterization of the largest cohort of patients with XLH reported to date from China, which will help in evaluating the applicability of emerging therapies for this disease in this ethnic group.

1. Introduction

X-Linked Hypophosphatemia (XLH, OMIM 307800) is the most prevalent form of heritable rickets, with an approximate incidence of 3.9–5/100,000 and a dominant inheritance pattern [1]. The genetic basis of XLH is loss-of-function mutations in the *PHEX* gene (Phosphate-regulating gene with Homology to Endopeptidases on the X chromosome) [2], which lead by a yet unknown cellular mechanism to overproduction of FGF23 by osteocytes [3,4]. Over 420 different *PHEX* mutations have been reported in the Human Gene Mutation Database (HGMD, http://www.uwcm.ac.uk/uwcm/mg/hgmd0.html, accessed November 2017), including small deletions/insertions, missense mutations, nonsense mutations, abnormal splicing patterns and gross insertions/deletions.

FGF23 is a critical regulator of phosphate and Vitamin D homeostasis. Excess FGF23 leads to chronic hypophosphatemia by reducing

* Corresponding author.
E-mail address: xiaweibo8301@163.com (W. Xia).

https://doi.org/10.1016/j.bone.2019.01.021
Received 16 November 2018; Received in revised form 11 January 2019; Accepted 20 January 2019
Available online 23 January 2019

renal phosphate reabsorption through suppression of expression of the renal tubular sodium phosphate co-transporters, as well as by increasing catabolism and decreasing synthesis of the active form of vitamin D, 1,25-dihydroxyvitamin D ($1,25(OH)_2D_3$) [5].

Clinical features of XLH include a waddling gait and rickets in childhood, and persistent osteomalacia in adults, lower-extremity deformities, bone pain, short stature, recurrent dental abscesses and enthesopathy (calcification of tendons and ligaments). Cardinal, biochemical abnormalities in XLH include life-long hypophosphatemia, normal to high PTH levels, inappropriately low-to-normal $1,25(OH)_2D_3$ and elevated serum alkaline phosphatase (ALP) [6,7]. XLH usually presents within the first year and a half of life as difficulty with ambulation and the appearance of rachitic deformities, usually first noticed in the lower extremities.

Until very recently, the therapeutic approach to this disease was to use active vitamin D metabolites and phosphate salts in an attempt to address the biochemical abnormalities. Although this therapy is efficacious, adherence is difficult with multiple daily doses, numerous side effects, and is not infrequently complicated by the appearance of hyperparathyroidism and nephrocalcinosis. Further, it does not correct the underlying pathophysiology of XLH.

A neutralizing antibody to FGF23, burosumab, was recently approved in the United States and Europe for the treatment of XLH. It corrects the underlying pathophysiology of XLH by neutralizing excess circulating FGF23 and thereby normalizing serum phosphate and correcting Vitamin D metabolism. It has shown impressive efficacy in phase 2 trials in children and in a recently reported RCT phase 3 trial in symptomatic adults with this disease [8,9]. Administered as a once or twice monthly subcutaneous injection, is vastly more convenient to administer and has far fewer side effects than conventional therapy.

Given this advance in XLH therapy, it now becomes of interest to better define the clinical spectrum of disease in under-studied populations. This report summarizes the experience at one major referral center in China, in a large cohort of patients with XLH.

2. Subjects and methods

2.1. Patients

This study is a retrospective review of 261 patients followed at Peking Union Medical College Hospital (PUMCH) from 2005 to 2017, who had clinical features of XLH and known or novel mutations in the *PHEX* gene. These included 126 familial cases and 135 sporadic cases, belonging to 216 unrelated pedigrees. The study was approved by the Department of Scientific Research, PUMCH. Prior to study participation, informed consent was obtained from all the patients, or from patients' parents if they were under 18 years old.

2.2. Clinical features

Since the purpose of the study was to characterize the presenting characteristics of patients with XLH in China, the data were collected only from patients at the time of their initial diagnosis and prior to any therapy, or from patients who had discontinued therapy for at least one year prior to the time of data collection. Medical records for all study subjects were reviewed and relevant data were extracted. Height measurements were converted to a standard deviation score (SDS) using standardized growth charts for Chinese children and adolescents ages 0 to 18 years [10]. Renal ultrasound was performed in 51 patients on their initial examination for the evaluation of nephrocalcinosis. Bilateral posteroanterior radiographs of wrists and knees were available for 47 subject patients with open epiphyses. A Rickets Severity Score (RSS) was evaluated for each of these patients using the method of Thacher [11]. The severity of rickets using this method is scaled from 0 (normal) to 10 (severe). Radiographs were read and scored independently by two physicians, and their scores averaged.

2.3. Biochemical analyses

Serum phosphate (P), total calcium (Ca) and alkaline phosphatase (ALP) were measured on an auto-analyzer (Beckman Coulter, America). Serum intact parathyroid hormone (i-PTH), 25-hydroxyvitamin D (25OHD) and β-isomerized C-terminal telopeptide of type I collagen (β-CTx) levels were measured using an automated Roche electrochemiluminescence system (Roche Diagnostics, Switzerland). Serum $1,25(OH)_2D_3$ was measured using an enzyme-linked immunoassay (DiaSorin, USA). Serum phosphate and ALP were compared to age and sex referents normative data [12].

2.4. Serum intact FGF23 (iFGF23) measurement

233 serum samples which were collected at the patient's initial visit to PUMCH were available for the iFGF23 measurement. Samples had all been stored at −80 °C until analysis. Serum iFGF23 levels were measured using a two-site ELISA kit (KAINOS Laboratories, Inc., Tokyo, Japan). The detectable concentration range of the iFGF23 using this assay is 3–800 pg/mL. The reference range for serum iFGF23 in our laboratory is 16.1 to 42.2 pg/mL (± 2SD from the mean) [13].

2.5. Analysis for PHEX gene mutations

Genomic DNA was extracted from 0.2 mL of whole blood using a commercial DNA extraction kit (QIAamp DNA Micro; Qiagen, Germany). PCR was performed on the 22 exons and > 50 bp of flanking intronic sequences of the *PHEX* gene, using 22 pairs of primers (Supplemental Table 1), which were designed using Primer Premier 6.0 software (PREMIER Biosoft International, Palo Alto, CA, USA). Direct DNA sequencing of PCR product was accomplished using an ABI 373XL sequencer (Applied Biosystems, Foster City, CA). Sequencing results were compared with the normal *PHEX* sequence available at UCSC genome bank (http://genome.ucsc.edu/). Novel mutations were defined as mutations that were neither included in the databases of HGMD, nor detected in 100 unrelated healthy Chinese individuals.

2.6. Multiplex Ligation-dependent Probe Amplification (MLPA) analysis

To detect large deletion/duplication mutations in the *PHEX* gene, Multiplex Ligation-dependent Probe Amplification (MLPA) analyses were performed on samples in which no mutations were detected by direct DNA sequencing. The MLPA analysis was performed according to the manufacturer's instructions (Salsa MLPA Kit P223 PHEX, Version.01, MRC-Holland, Amsterdam, Netherlands) and the product analyzed using the ABI 3730XL sequencer (Applied Biosystems, Foster City, CA) and the Coffalyser software program (MRC-Holland, Amsterdam, Netherlands).

2.7. Homology modeling of PHEX protein structure and location of identified PHEX missense and nonsense mutations

Since the three-dimensional (3D) protein structure of PHEX has not yet been solved, and to better visualize the location of the identified mutations distribution, SWISS-MODEL was used to construct a putative 3D model of the PHEX protein based on the crystal structure of Neprilysin (NEP, PDB ID: 5JMY), the closest homolog of PHEX in the M13 peptidase family to which PHEX belongs. In this homology model, just as in the NEP crystallographic structure, amino acids 1–53 containing the intracellular and transmembrane regions are not represented. All missense and nonsense mutations detected in this study as well as previously reported were positioned on the PHEX model using open source software (PyMol; https://pymol.org/2/).

2.8. Genotype-phenotype correlation

Phenotypic characteristics included in sex difference and the genotype-phenotype analyses were age of presentation, age of first walk, age at which lower limb deformities were first noticed, height SDS, iFGF23 levels, and RSS. In an effort to correct for the impact of age and gender on phosphate measurements in the genotype-phenotype correlation, we used the "serum phosphate/upper limit ratio". This measurement was calculated by dividing each patient's serum phosphate by the upper limit of normal for serum phosphate for that patient's age and gender. *PHEX* mutations were classified as plausible truncating mutations (nonsense, frame-shift insertions/deletions and splice site mutations), or non-truncating mutations (missense and in-frame insertions/deletions) based on previous studies by Holm et al. [14]. Mutations were considered to be N-terminal if they occurred between aa 1–649, or C-terminal if they occurred between aa 650–749 as described by Holm et al. [14].

2.9. Statistical analyses

Statistical analyses were conducted using SPSS for Windows version 19.0 (SPSS Inc., Chicago, IL). The Kolmogorov-Smirnov test was used to determine the distribution of continuous variables. Normally distributed continuous variables are presented as mean ± SD and compared by Student's *t*-test. Non-normally distributed continuous variables, are presented as median (25th, 75th percentiles), and compared by Mann-Whitney *U* test. Spearman's rank correlation coefficient analysis without adjustment was used to evaluate correlations between parameters. A P value < 0.05 was considered statistically significant.

3. Results

3.1. Clinical features and biochemical parameters of XLH patients

The study cohort consisted of 261 patients (84 males, 177 females), aged 5 months to 58 years (median age 10 years). Patients represented 216 pedigrees and included 126 familial cases and 135 apparently sporadic cases. Table 1 summarizes the presenting of complaints at the time of initial evaluation. The average age at presentation was 15 months (12, 24; 25th, 75th percentile; N = 174). 78.0% of patients presented with lower limb bowing or difficulty in ambulation. Patients had delayed ambulation, with walking first noted at an average age of 15 months (12, 18; N = 150). Tooth eruption was also delayed to an average age of 7.5 months (6, 8.4; N = 100). In this cohort, 104 patients had previously received treatment with oral phosphate and calcitriol, while 36 patients had received oral phosphate or calcitriol alone for variable lengths of time. The average age at initiation of therapy of our cohort was 3 years (2, 5; N = 132).

Table 1
Presenting clinical complaints at initial evaluation.

	Percentage (%)
Bowed lower extremities	47.0%
Waddling gait, muscle weakness, repeated falling	29.0%
Short stature, growth retardation	6.0%
Central skeletal and dermatologic complaints[a]	5.7%
Lower extremities bone or joint pain	4.2%
Dental problems[b]	3.9%
Delayed walking	2.1%
Family history[c]	2.1%

[a] Rickets manifestations including frontal bossing, occipital alopecia, pectus carinatum, pectus excavatum, rachitic rosary.
[b] Dental problems including delayed dentition, enamel hypoplasia dental abscess or abnormal loss of teeth at an early age.
[c] Family history indicates patients first came to the clinic for disease screening since their parents or siblings were diagnosed with XLH. These patients came to the clinic at an early age (5 to 10 months) without any obvious signs or symptoms showing up.

Table 2
Biochemical parameters in our study cohort.

	XLH patients	Sample number (N)	Reference range (age/sex)
Ca (mmol/L)	2.35 ± 0.13	145	2.13–2.7
P (mmol/L)	1.03 (0.85, 1.04)	5	1.55–2.65 (< 1 yr)[a]
	0.80 ± 0.12	37	1.25–2.1 (1–3 yr)
	0.81 (0.74, 0.85)	30	1.2–1.8 (4–11 yr)
	0.83 ± 0.14	13	0.95–1.75 (12–15 yr)
	0.61 ± 0.10	54	0.9–1.5 (> 15 yr)
ALP (U/L)	593.5 (476.3, 770.0)	80	42–390 (0–15 yr)[b]
	444.3 ± 203.3	7	52–171 (16–18 yr)
	150.0 ± 33.3	8	45–125 (> 19 yr/M)
	98.0 (76.3, 142.5)	36	35–100 (19–49 yr/F)
	106.0, 153.0[c]	2	50–135 (> 50 yr/F)
25OHD (ng/mL)	15.9 (11.6, 22.7)	63	7.9–32.6 [15]
$1,25(OH)_2D_3$ (pg/mL)	44.2 ± 18.7	39	19.6–54.3
i-PTH (pg/mL)	72.3 (52.4, 94.0)	103	12–68
β-CTx (ng/mL)	0.70 (0.40, 1.69)	40	0.21–0.44
Cr (μmol/L)	41.1 ± 15.1	94	
24hUCa (mmol/24 h)	1.20 (0.73, 2.53)	48	< 6.25 (F)
	0.91 (0.33, 2.13)	31	< 7.5 (M)
24hUP (mmol/24 h)	13.9 (10.1, 19.0)	79	
iFGF23 (pg/mL)	101.9 (71.4, 143.8)	233	29.15 ± 13.09[d]

Abbreviations are as follows: *Ca* serum calcium, *P* serum phosphate, *ALP* serum alkaline phosphatase, *25OHD* serum 25-hydroxyvitamin D, $1,25(OH)_2D_3$ serum 1,25-dihydroxyvitamin D, *i-PTH* serum intact parathyroid hormone, *β-CTx* serum β-isomerized carboxyl-terminal telopeptide of type I collagen, *Cr* serum creatinine, *24hUCa* 24-hour urinary calcium, *24hUP* 24-hour urinary phosphate, *iFGF23* serum intact fibroblast growth factor 23, *yr* year(s), *M* male, *F* female.
[a] Serum phosphate reference ranges according to age subgroups [12].
[b] Serum alkaline phosphatase reference ranges at the central laboratory of Peking Union Medical College Hospital.
[c] Only two ALP values were available (106 U/L and 153 U/L) in the > 50 yr/F subgroup and were directly listed in Table 1.
[d] Reference range for the iFGF23 was determined in our own laboratory from 8 healthy controls (Mean ± 2SD) [13].

Table 2 summarizes the biochemical findings in our cohort. Serum phosphate was below the lower limit of normal range in all age groups. ALP was also above the upper limit in all age and sex subgroups except in females over the age of 19 in whom values were in the high-normal range. Serum and urine calcium on average were within the normal range but i-PTH was slightly elevated. Serum $1,25(OH)_2D_3$ levels were within the normal range, while 25OHD levels could be considered low or low-normal depending on the reference range chosen [15].

At the time of evaluation, 96.4% of patients for whom data were available (N = 139) were frankly hypophosphatemia, the remaining 5 patients had values at the lower limit of normal. Serum ALP levels were apparently elevated in 78.2% of the whole patient population (N = 133). Nearly 91% of children and adolescents (no more than 18 years, N = 87) presented with a high serum ALP. Mean serum β-CTx was quite elevated likely reflecting underlying severe metabolic bone disease.

3.2. IFGF23 levels in XLH patients

IFGF23 levels varied widely in the study cohort and were abnormally distributed, ranging from 6.46 to 542.57 pg/mL, with a median value of 101.9 pg/mL (Table 2). 91.9% of patients had a serum iFGF23 level above the upper limit of the reference range. Interestingly, serum iFGF23 levels did not correlate with serum phosphate/upper limit ratio, age at which disease symptom developed, height SDS, or RSS (data not

Table 3
Skeletal abnormalities, heights and RSS on initial examination.

	Percentage % (case number)
Lower limb deformity[a]	95.9% (208/217)
Genu varum	77.4% (161/208)
Genu valgum (knock knees)	11.5% (24/208)
Complex deformity	5.8% (12/208)
Thoracocyllosis	
Pectus carinatum	35.6% (67/188)
Rachitic rosary	72.1% (137/190)
Thickened ankles and wrists	70.3% (121/172)
Height (SDS)	−2.7 ± 1.6 (N = 167)
Juveniles (height SDS)	−2.4 ± 1.5 (N = 117)
Adults (height SDS)	−3.5 ± 1.4[b] (N = 50)
RSS[c]	6.0 (5.0, 7.0) (N = 47)

[a] 11 patients were recorded with only lower limb deformity in their medical records, without depicting any details of the deformities.
[b] Significant difference in height SDS exists between juveniles (< 18 yrs) and adults (≥18 yrs) (P = 0.00).
[c] RSS: Rickets Severity Score; data present as median (25th, 75th percentile).

shown).

3.3. Skeletal abnormalities

The vast majority of patients had markedly short stature. The average height SDS was −2.7 ± 1.6 (N = 167), with 67.7% of patients less than −2 SD (Table 3). Adults showed an even greater impairment in height compared with younger patients (mean height SDS values: −3.5 ± 1.4 vs −2.4 ± 1.5; N = 50 and 117, respectively; P < 0.001; Table 3). A negative correlation between height SDS and age at initiation of therapy was observed in our cohort (r = −0.213, P = 0.029, N = 105). However, no correlation was observed between serum phosphate levels and height SDS (data not shown).

Table 3 summarizes the skeletal findings in the study cohort. Lower limb deformities were the most common abnormalities found on physical examinations and were present in 95.9% patients. Genu varum was the single most prevalent lower limb deformity. Indicative of severe disease, > 70% of patients had either a rachitic rosary or thickened ankles and wrists. In 47 subjects, for whom radiographs were available, the median RSS was 6 points (range 4–10) also indicative of severe rickets in these patients. Radiographs from a 2-year old girl with severe rickets (RSS 10 points) are shown in Fig. 1.

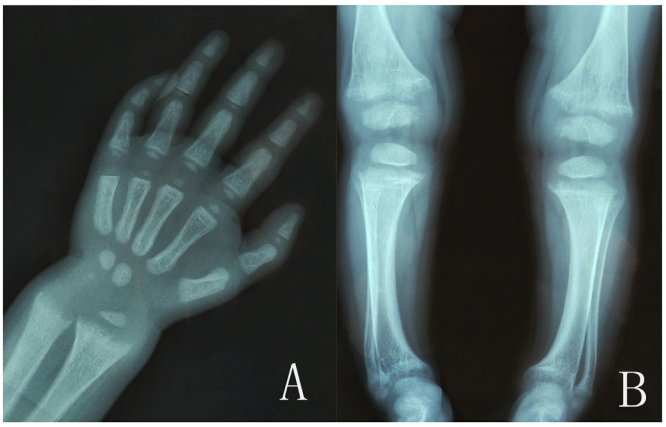

Fig. 1. Radiographs of the left wrist and both knees of a 2-year-old girl with severe rickets (RSS = 10 points). (A) The wrist shows metaphyseal concavity with fraying of the end-plates in both the radius and ulna (wrist RSS = 4). (B) In both femurs and tibiae, there is complete lucency in the zone of provisional calcification. The epiphyses are widely separated from distal metaphyses (knee RSS = 6).

Table 4
Mutation numbers and frequencies of different types of *PHEX* mutations.

Mutation types	Mutation numbers	Percentage (%)
Point mutations		
Missense mutations	25	15.1%
Nonsense mutations	36	21.7%
Splice site mutations	26	15.7%
Insertions	24	14.5%
Deletions	31	18.7%
Large insertions/deletions	24	14.5%
Total mutations	166	100%

3.4. Renal calcifications

Very few of study subjects had ultrasonographic evidence of nephrocalcinosis or nephrolithiasis (1.96%; N = 51).

3.5. Mutational analysis of PHEX gene

PHEX gene mutational analysis of the 261 XLH patients (from 216 pedigrees) revealed 166 different mutations, including 142 point mutations and 24 large insertions/deletions (Table 4, Fig. 2). One hundred and eleven of the 166 mutations (66.3%) had not been previously reported. These included 15 missense, 17 nonsense, 15 splicing mutations, 26 deletions, 20 insertions and 18 large insertions/deletions. Mutation frequencies were analyzed by pedigrees (N = 216), rather than by individual, except obviously in sporadic cases. All of *PHEX* mutations found in the present study or previously reported by other studies were summarized in Supplemental Table 2.

The 142 point mutations, detected in 187 pedigrees, were distributed throughout the *PHEX* coding sequence and flanking intronic sequences, and even included the N-terminal (p.M1V) and C-terminal amino acids (p.X750Q) (Fig. 3). Mutations were more frequent in the 3′ region of *PHEX* gene (54.6%; exons 15–22 and adjacent introns). Within these 8 exons, exons 15, 20, 18 and 17 with their flanking regions had higher point mutation frequencies (Fig. 3B). Among all the point mutations, P534L, G579R, R747X and c.1645+1 G > A were the most frequent (3.69%, 3.23%, 3.23% and 3.23%, respectively), which seem to be the hotspot mutations of *PHEX* gene. Six mutations (C54X, C77W, C85Y, C85S, C406S, C693Y) occurred at highly conserved cysteines. Interestingly, two unrelated male patients were found to be mosaics (c.1645+4A > G, c.933+1G > A; Fig. 4) with a height SDS of −1.98 and −0.92, respectively.

3.6. Mutation distribution in a 3D level of homology modeling PHEX protein

To help visualize the distribution of the 83 missense and 74 nonsense *PHEX* mutations identified in the present study and previously reported, we constructed a 3D model of the PHEX protein based on its homology to another M13 gene family member, Neprilysin (NEP), as described in the Methods. As illustrated in Fig. 5A, nonsense mutations were fairly evenly distributed throughout the protein. Since nonsense mutations lead to synthesis of a truncated protein which likely is rapidly degraded, they provide no insights into regions of the PHEX protein that may have functional significance. Fig. 5B illustrates the distribution of missense mutations, which are concentrated in the two putative lobes of the PHEX protein. The substrate for PHEX has not yet been identified, and the molecular anatomy of the catalytic site of PHEX is unknown. However, the catalytic site of NEP occupied by the inhibitor phosphoramidon has been resolved [16]. The exons in NEP that form part of its catalytic site surrounding the zinc binding domain and that contain the amino acids that directly interact with phosphoramidon, are exons 16, 17, 19 and 20. The corresponding functional exons in PHEX are exons 15, 17, 19 and 20. Interestingly, 51.2% of missense mutations identified in this study were located in these four

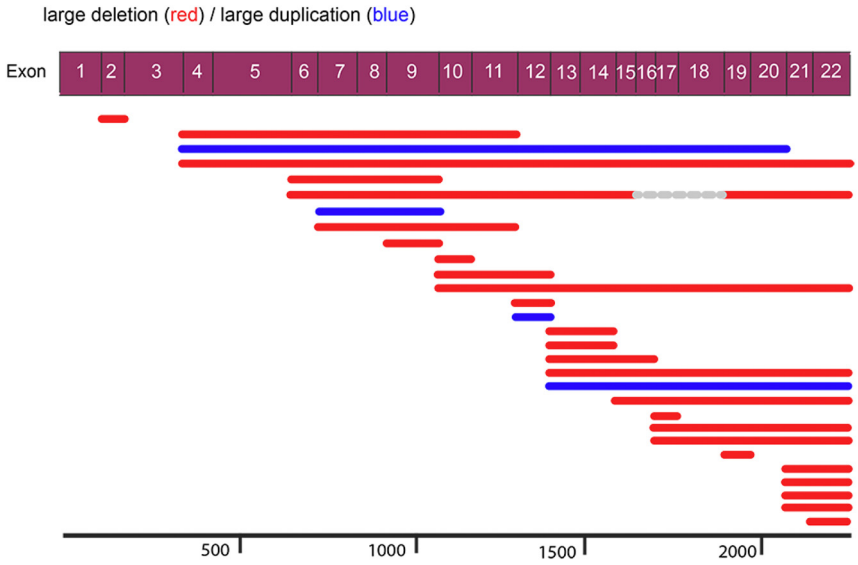

Fig. 2. Large deletions/duplications in *PHEX* identified in the study cohort. Twenty different large deletions and four large duplications of the *PHEX* gene were found in 25 and 4 XLH pedigrees, respectively. Red represents deletions; blue represents duplications. (For interpretation of the references to color in this figure legend, the reader is referred to the web version of this article.)

exons. Furthermore, 20.9% of missense mutations found in the present study occurred within the amino acids that correspond to those in NEP that directly interact with phosphoramidon and presumably are important for both enzymes catalytic activity (aa 539, 540, 567–586, and 641–666). In the aggregate, these findings suggest that exons 15, 17, 19 and 20 and the amino acids just mentioned, are functionally important in PHEX, since disease-causing mutations are enriched in these domains of the molecule.

3.7. Sex differences and genotype-phenotype correlation

Sex differences and genotype-phenotype correlations were analyzed using the data from this large cohort. Although based on an X-linked dominant inheritance pattern, it might be assumed that males would have a more severe phenotype than females, there were no significant sex differences in any of the measured clinical or biochemical parameters. There was a trend toward a slightly lower height in males that did not reach statistical significance (P = 0.078 for SDS) (Table 5).

There were no phenotypic differences between patients with truncating and non-truncating mutations. In previous studies, genotype-phenotype correlations have contrasted phenotype correlations with disease-causing variants in the first 649 amino acids to phenotype correlations with mutations in the rest of the molecule [14]. We therefore conducted a similar analysis. Patients with mutations in the first 649 (of 749 amino acids) presented with signs and symptoms at an earlier age (P = 0.015) and had higher circulating levels of iFGF23 (P = 0.045) compared to patients with mutations in the rest of the PHEX protein. Despite an earlier age of symptomatic onset and higher FGF23 levels, there were no differences in other biochemical or phenotypic characteristics in these two groups (Table 6).

4. Discussion

The present study provides a robust and detailed characterization of untreated individuals with XLH in China. This is the largest single site study of XLH to be reported to date from any institution. In brief our patients displayed all of the typical manifestations of this disease, leading us to conclude that in China the disease presents and progresses much like it does in Western nations, where most of the published work on this disease has been conducted.

As is typical in XLH, our pediatric patients first came to clinical attention early in life (median age 15 months). They presented with lower limb deformities and weakness, short stature/growth retardation, and other classical signs of rickets (e.g. rachitic rosary, pectus carinatum, and thickened wrists/ankles). Most of our patients have a slight delay in walking unassisted with a median age of 15 months. 96.4% of our study subjects were hypophosphatemic for age, and on average had significantly elevated circulating levels of iFGF23. Despite normal serum calcium values, PTH levels were elevated as is often the case in untreated XLH as noted above. Because FGF23 markedly induces CYP24A1, the enzyme that catabolizes $1,25(OH)_2D_3$, and inhibits CYP27B1, the enzyme that converts 25OHD to the active metabolite, serum levels of $1,25(OH)_2D_3$ were low or inappropriately normal for the degree of hypophosphatemia and secondary hyperparathyroidism [5]. Indicative of a severe defect in mineralization, serum ALP levels were elevated.

The mean height SDS of -2.7 ± 1.6 in our cohort is consistent with other published reports quantifying short stature in XLH, with SDS values ranging from -0.9 to -2.48 [17–20]. Adults in our cohort had more severe short stature compared with younger patients likely due to a life-time of untreated disease.

The biochemical findings are also very typical of those reported in untreated patients with XLH in the West [21]. Serum iFGF23 levels varied considerably in this study cohort (ranging from 6.46 to 542.6 pg/mL), but 91.8% had values above the upper-limit of the reference range (42.2 pg/mL). Previous studies have reported iFGF23 levels to be 5–10 folds higher in XLH compared to normal [4,22]. Although recent work has suggested that FGF23 may directly affect bone mineralization independent of its phosphaturic properties [23,24], we found no correlation between iFGF23 levels and age at presentation, height, or rickets severity.

Elevated serum PTH levels were detected in 59.2% in this cohort (N = 61/103). This is consistent with previous reports of secondary hyperparathyroidism in treatment naïve XLH individuals [17,25]. A number of factors may play a role in secondary hyperparathyroidism in this disease, including low circulating levels of $1,25(OH)_2D_3$ limiting the ability of this metabolite to suppress PTH levels. In addition, 25OHD deficiency can contribute to this phenomenon. Our patient population had relatively low 25OHD levels. Finally, extensive osteomalacia may limit the ability of PTH to induce the resorption of mineralized bone in support of normal calcium thereby engendering secondary hyperthyroidism.

PHEX consists of 22 exons, spanning 2247 bp and encodes a 749-amino-acid transmembrane endopeptidase, that belongs to the M13 zinc metallopeptidases family, which includes Neprilysin (NEP), endothelin-converting enzymes (ECE-1 and ECE-2), the KELL blood group antigen and damage-induced neuronal endopeptidase (DINE)/X-converting enzyme (XCE) [26,27]. Some genomic structures are conserved

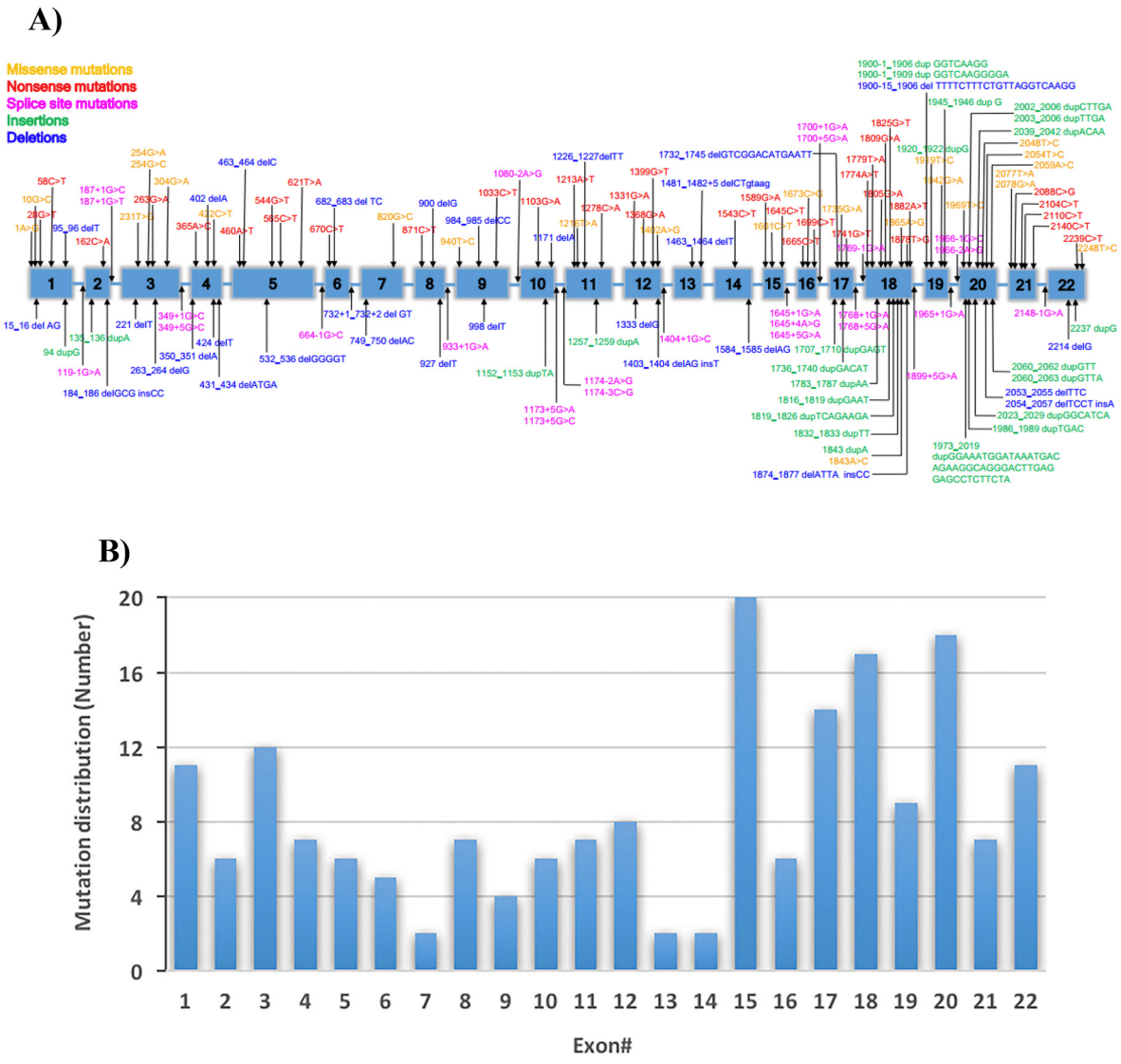

Fig. 3. A. Distribution of all point mutations identified in the present study. The 142 different point mutations (including missense mutations, nonsense mutations, splice site mutations and small insertions/deletions) were distributed across the 22 exons and the adjacent intron areas of the *PHEX* gene. Yellow represents missense mutations; red represents nonsense mutations; pink represents splice site mutations; green represents small insertions; blue represents small deletions.
B. Distribution of point mutations within the 22 exons and the adjacent introns of *PHEX* gene. Exon 15, 20, 18 and 17 had higher point mutation frequencies than any of the other exons, with a mutation frequency of 10.70% (N = 20), 9.63% (N = 18), 9.09% (N = 17) and 7.49% (N = 14), respectively, among the 187 pedigrees in which the point mutations were identified. 54.6% of the point mutations occurred in the 3′ region of *PHEX* (exons 15 to 22). (For interpretation of the references to color in this figure legend, the reader is referred to the web version of this article.)

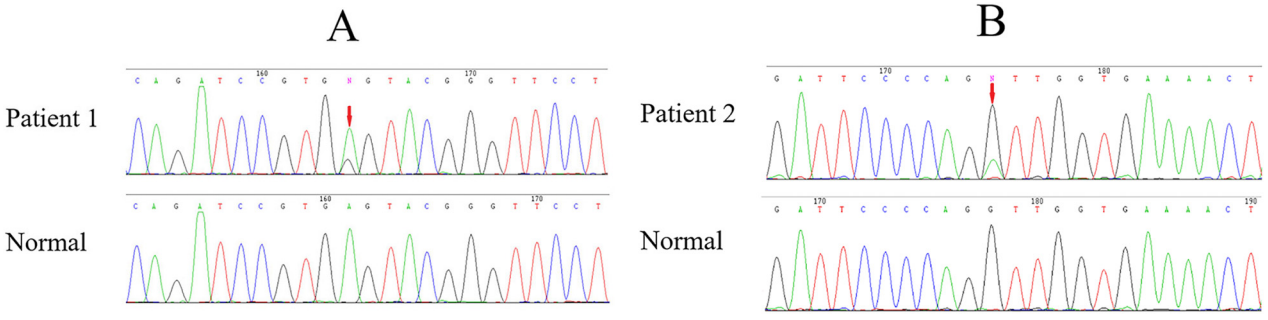

Fig. 4. Mutational analysis of *PHEX* gene revealed two mosaic mutations in two unrelated male XLH patients. (A) Sanger sequencing revealed a splice site mutation c.1645+4 A > G of *PHEX* gene in a 10-year-old male patient. Red arrow indicates two peaks at the site c.1645+4: one peak is a wild-type A and the other is substituted to G. (B) Sanger sequencing revealed a splice site mutation c.933+1 G > A of *PHEX* gene in a 3.5-year-old male patient. Red arrow indicates the mutation site: one peak is a wild-type G and the other is substituted to A. (For interpretation of the references to color in this figure legend, the reader is referred to the web version of this article.)

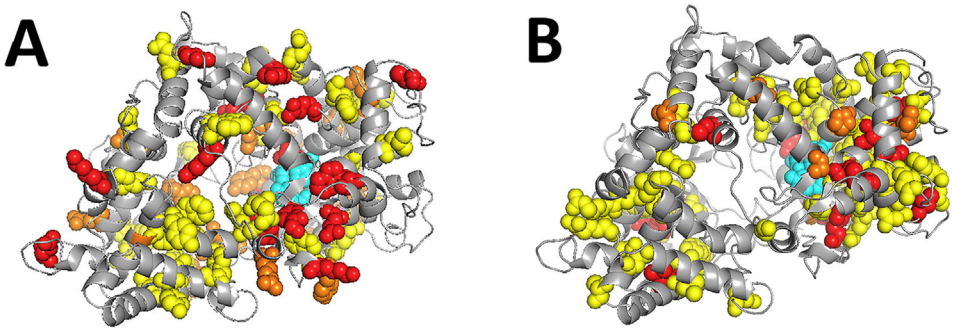

Fig. 5. Distribution of missense/nonsense mutations in a 3D model of the PHEX protein. The 3D model of PHEX was constructed based on the crystal structure of neprilysin (NEP, PDB ID: 5JMY). (A) Nonsense mutations were fairly evenly distributed throughout the 3D PHEX model. (B) Missense mutations were mainly located within the two putative lobes of the PHEX protein, and especially clustered near the zinc-binding site (shows as cyan spheres), which is an important functional region of PHEX. Red spheres represents mutations first reported in the present study; orange represent the mutations that were both identified in the present study and previously reported; yellow represent other missense/nonsense mutations that have been previously reported but not identified in the current study. (For interpretation of the references to color in this figure legend, the reader is referred to the web version of this article.)

among all M13 family members, including a short N-terminal cytoplasmic domain, a single transmembrane domain and a large extracellular C-terminal domain (which contains the zinc-binding motifs and ten conserved cysteine residues) [28]. The zinc-binding motifs, located on exons 17 and 19, are essential for the catalytic activity of PHEX protein [29]. The cysteine residues likely play an important role in the protein structure formation, including disulfide-bond formation and protein folding [30].

In our cohort of 261 patients, 166 different *PHEX* mutations (include missense mutations, nonsense mutations, small insertions/deletions, splice site mutations and large insertions/deletions) were identified. Of the 166 mutations, 55 had been previously reported and 111 were novel (66.9%). The majority of the *PHEX* mutations (84.94%) were predicted to lead to truncation of the PHEX product, including nonsense and frameshift insertions/deletions, splicing mutations, and large insertions/deletions.

Mutations were scattered throughout the 22 exons and the adjacent intronic areas of the *PHEX* gene. We found a slightly greater proportion of gross insertions/deletions compared with Human Gene Mutation Database (14.5% vs. 9.5%). It is possible that the higher detected frequency of gross deletions/duplications in this study resulted from the use of MLPA analysis. Various studies have reported that MLPA analysis increases the rate of detection of *PHEX* mutations in hypophosphatemic rickets patient cohorts from 45.6% - 79% by direct sequencing to 83.3% - 84.6% [14,31–37].

Similar to previous reports [34,38,39] we found a higher proportion of mutations in the C-terminal portion of the molecule and in particular, in the current study exons 15, 17, 18 and 20 each had more mutations per exon than any of the other 22 exons. Interestingly the C-terminal portion of PHEX shares the greatest sequence identity with the other M13 family members, and as noted contains the zinc-binding domains [29]. Of the missense mutations identified in the current study, 80% were found in the 220 most highly conserved amino acids in PHEX [29], suggesting that each of these plays a critical role in the PHEX function (Supplemental Table 3).

The crystal structure of the M13 family member, NEP, has been reported [16]. NEP has a large central cavity which encompasses the catalytic site. A similar structure is observed in the 3D PHEX protein model (Fig. 4). Interestingly, we found that missense mutations, but not nonsense mutations, were clustered in the two putative lobes of our 3D PHEX protein model, especially around the zinc-binding regions. Corresponding to NEP genomic structure, exons 15, 17, 19 and 20 in PHEX would be predicted to contribute to its catalytic zinc binding domain based on our 3D model. In the aggregate, these findings suggest that exons 15, 17, 19 and 20 are important functional regions of PHEX, since missense mutations are enriched in these domains of the molecule, and single amino acid substitutions in these genomic regions result in a non-functional protein. A similar result was reported by Gaucher et al. [32].

In addition, as noted in the Results, we found that 4 point mutations in *PHEX* occurred with fairly high frequency in our cohort, confirming reports by others that these are likely mutational hot spots [25,29,30,32,37,38]. Also consistent with other reports [14,31,32,37,38], of the substitution mutations, P534L was the most prevalent. P534 is predicted to be adjacent to the active site of the enzyme, and predicted to interrupt local hydrophobicity since a hydrophobic leucine is substituted for a neutral proline [31,37]. The G579R, mutation occurs next to the highly conserved zinc-binding motif ^{580}HEXXH^{584}, which might interfere with its catalytic activity [40]. The mutation G579R also can result in a protein that cannot be terminally glycosylated and thereby trapped in the endoplasmic reticulum [41].

In addition, 6 mutations (C54X, C77W, C85Y, C85S, C406S, C693Y) were located in 5 of the 10 highly conserved cysteine residues of PHEX. Cysteine residues are required for disulfide-bond formation, which is critical to tertiary protein structure of PHEX [30].

Nonsense mutations and splice site mutations are considered to lead to a truncated and dysfunctional protein. One of these, R747X, was associated with a stop codon appearing only three amino acids proximate to the C-terminus, suggesting that even the last 3 amino acids are important for PHEX function.

We also identified two mosaic XLH patients, with a rare occurrence. Two splice site mutations (c.1645 + 4A > G, c.933 + 1G > A) were detected in two unrelated male XLH patients, respectively. Given that the detection of these mutations was accomplished using peripheral blood

Table 5
Sex difference in XLH patients.

	Males	Sample number (N)	Females	Sample number (N)	P value
Serum Phosphate/upper limit ratio	0.42 ± 0.09	46	0.41 ± 0.06	93	0.251
Age when signs and symptoms were first noticed[a]	15 (12, 24)	60	15 (12, 21)	114	0.284
Age when first walked unassisted[a]	15 (12, 18)	55	15 (12, 18)	95	0.844
Age when lower limb deformity first appear[a]	18 (12, 24)	46	16 (12, 31.5)	78	0.817
Height (SDS)	−3.0 ± 1.6	59	−2.6 ± 1.6	108	0.094
RSS	7 (6, 7)	19	6 (5, 8)	28	0.850
iFGF23 (pg/mL)	109.8 (73.8, 149.3)	72	98.4 (71.6, 140.5)	158	0.696

[a] Ages are displayed in months.

Table 6
Genotype-phenotype correlation in XLH patients.

	Truncating mutations	Non-truncating mutations	P value	N-terminal mutations (from 5′ end to 649AA)	C-terminal mutations (from 650AA to 3′ end)	P value
Serum phosphate/ Upper limit ratio	0.41 ± 0.08 (N = 107)	0.42 ± 0.06 (N = 32)	0.674	0.41 ± 0.07 (N = 113)	0.42 ± 0.09 (N = 26)	0.573
Age when signs and symptoms were first noticed[a]	15 (12, 24) (N = 143)	16 (12, 24) (N = 31)	0.641	16 (12, 24) (N = 141)	14 (12, 18) (N = 33)	0.015
Age when first walked unassisted[a]	15 (12, 18) (N = 121)	15 (14, 18) (N = 29)	0.235	15 (12, 18) (N = 119)	14 (12, 18) (N = 31)	0.478
Age when lower limb deformity first appear[a]	17.5 (12, 24) (N = 106)	21 (13.5, 36) (N = 18)	0.312	18 (12, 36) (N = 104)	14.5 (12, 18) (N = 20)	0.055
Height SDS	−2.80 ± 1.62 (N = 133)	−2.53 ± 1.45 (N = 34)	0.379	−2.77 ± 1.62 (N = 132)	−2.65 ± 1.45 (N = 35)	0.692
RSS (Rickets Severity Score)	6.5 (5, 7) (N = 42)	6.2 ± 1.3 (N = 5)	0.724	7 (5, 7) (N = 37)	6.4 ± 1.7 (N = 10)	0.711
iFGF23 (pg/mL)	102.4 (74.5, 140.2) (N = 184)	96.2 (63.3, 171.3) (N = 49)	0.777	102.9 (78.3, 152.6) (N = 187)	92.4 (54.8, 134.4) (N = 46)	0.045

[a] Ages are displayed in months.

leukocyte DNA, somatic mosaicism must have resulted from a spontaneous mutation at an early postzygotic division. The heights (SDS) of these two patients were −1.98 and −0.92, respectively, compared to the non-chimeric male patients who had a mean height of −3.1 ± 1.6 (N = 57). In addition, they had less skeletal disease and presented at an older age, all of which suggests that they were more mildly affected. A gene dosage-effect has been posited in mosaic XLH patients with the severity of disease dependent on the ratio of normal to mutant allele [42]. It should be noted that mosaicism is difficult to detect by Sanger sequencing in females.

Considerable controversy exists regarding whether male patients are more severely affected than females due to the gene dosage effect of X-linked dominant inheritance pattern [14,17–19,43–46]. In our large cohort there were no significant differences in age of presentation, height, rickets severity, serum phosphate/upper limit ratio, or iFGF23 levels based on sex although there was a non-significant trend toward lower heights in males (P = 0.078). However, Whyte et al. proposed that the sex differences of skeletal disease in XLH patients were more like to be ascribed to differing sex hormones or physical activities rather than gene dosage effect [43]. Another area of uncertainty is whether there is a genotype-phenotype correlation in XLH patients [14,19,25,47]. Heterogeneity of clinical manifestations was also a common finding in XLH patients due to the phenotypic variation in patients who carried identical *PHEX* mutations [36]. We thereby performed genotype-phenotype correlation in our cohort. Mutations were categorized by type and location in undertaking a genotype-phenotype analysis. No statistically significant correlation was found between mutation type and phenotype. However, patients with mutations in the first 649 aa of the molecule presented at an early age and had higher iFGF23 levels compared to those with mutations from aa 650 to 749.

A major strength of the current study is the large cohort size. It is the largest from China and the largest yet to be reported. It provides a comprehensive picture of XLH in China. It also robustly substantiates the findings of early studies regarding clinical presentation, and the lack of sex differences or of genotype-phenotype correlations. 166 different *PHEX* mutations were revealed in the current study, among which 111 were novel mutations. These findings largely augment the *PHEX* mutational spectrum, especially in the Chinese population. As in any retrospective study there were some limitations. Not all clinical or biochemical data were available for all patients. Although the first-line treatment for XLH is phosphate salts and calcitriol, the new therapy with the blocking antibody to FGF23 is persuasive given its efficacy and convenience. Since XLH in China shares all of the key clinical biochemical and genetic features of the disease in the West, it is likely that the FGF23 antibody, recently approved in Europe and the United States for the treatment of XLH, would also be efficacious in addressing this disease in China. The prevalence of XLH in China is not known but it is likely that there are large numbers of untreated and/or inadequately treated patients with XLH in China who could potentially benefit from this therapy. Therefore characterizing the pharmacokinetics and pharmacodynamics of this drug in a cohort of Chinese with XLH would be an important near -term goal.

Disclosures

All authors state that they have no conflicts of interest.

Acknowledgments

We appreciate the patients for their participation. This study was supported by the National Science and Technology Major Projects for New Drugs Innovation and Development (No. 2008ZX09312-01), the National Natural Science Foundation of China (No. 81170805, 81471088, 81670714), the National Key Program of Clinical Science (No. WBYZ2011-873), the Beijing Natural Science Foundation (No. 7121012). CAMS Innovation Fund for Medical Sciences (No. 2016-I2M-3-003).

Authors' roles

Dr. CZ, ZZ, YS, LX, RJ, KI and WX designed the study and prepared the first draft of the paper. Dr. CZ, ZZ, YS, LX, QP and MN contributed to the experimental work. Dr. CZ, LC and WX were responsible for data analysis and interpretation. Dr. YJ, ML, OW, XH, SH, XX, XM, XZ, LY and WX were responsible for clinical data collection. All listed authors revised the paper critically for intellectual content and approved the final version of the submitted manuscript. All authors agree to be accountable for the work and to ensure that any questions relating to the accuracy and integrity of the paper are investigated and properly resolved.

Appendix A. Supplementary data

Supplementary data to this article can be found online at https://doi.org/10.1016/j.bone.2019.01.021.

References

[1] S.S. Beck-Nielsen, B. Brock-Jacobsen, J. Gram, K. Brixen, T.K. Jensen, Incidence and prevalence of nutritional and hereditary rickets in southern Denmark, Eur. J. Endocrinol. 160 (2009) 491–497.
[2] F. Francis, S. Hennig, B. Korn, R. Reinhardt, P. de Jong, A. Poustka, H. Lehrach, P.S.N. Rowe, J.N. Goulding, T. Summerfield, R. Mountford, A.P. Read, E. Popowska, E. Pronicka, K.E. Davies, J.L.H. O'Riordan, M.J. Econs, T. Nesbitt, M.K. Drezner,

C. Oudet, S. Pannetier, A. Hanauer, T.M. Strom, A. Meindl, B. Lorenz, B. Cagnoli, K.L. Mohnike, J. Murken, T. Meitinger, A gene (PEX) with homologies to endopeptidases is mutated in patients with X–linked hypophosphatemic rickets, Nat. Genet. 11 (1995) 130–136.
[3] L.F. Bonewald, M.J. Wacker, FGF23 production by osteocytes, Pediatr. Nephrol. 28 (2013) 563–568.
[4] Y. Yamazaki, R. Okazaki, M. Shibata, Y. Hasegawa, K. Satoh, T. Tajima, Y. Takeuchi, T. Fujita, K. Nakahara, T. Yamashita, S. Fukumoto, Increased circulatory level of biologically active full-length FGF-23 in patients with hypophosphatemic rickets/osteomalacia, J. Clin. Endocrinol. Metab. 87 (2002) 4957–4960.
[5] T. Shimada, H. Hasegawa, Y. Yamazaki, T. Muto, R. Hino, Y. Takeuchi, T. Fujita, K. Nakahara, S. Fukumoto, T. Yamashita, FGF-23 is a potent regulator of vitamin D metabolism and phosphate homeostasis, J. Bone Miner. Res. 19 (2004) 429–435.
[6] T.O. Carpenter, E.A. Imel, I.A. Holm, D.B.S.M. Jan, K.L. Insogna, A clinician's guide to X-linked hypophosphatemia, J. Bone Miner. Res. 26 (2011) 1381–1388.
[7] T.O. Carpenter, The expanding family of hypophosphatemic syndromes, J. Bone Miner. Metab. 30 (2012) 1–9.
[8] T.O. Carpenter, M.P. Whyte, E.A. Imel, A.M. Boot, W. Hogler, A. Linglart, R. Padidela, H.W. Van'T, M. Mao, C.Y. Chen, A. Skrinar, E. Kakkis, M.J. San, A.A. Portale, Burosumab therapy in children with X-linked hypophosphatemia, N. Engl. J. Med. 378 (2018) 1987–1998.
[9] K.L. Insogna, K. Briot, E.A. Imel, P. Kamenicky, M.D. Ruppe, A.A. Portale, T. Weber, P. Pitukcheewanont, H.I. Cheong, D.B.S. Jan, Y. Imanishi, N. Ito, R.H. Lachmann, H. Tanaka, F. Perwad, L. Zhang, C.Y. Chen, C. Theodore-Oklota, M. Mealiffe, M.J. San, T.O. Carpenter, A randomized, double-blind, placebo-controlled, phase 3 trial evaluating the efficacy of burosumab, an anti-FGF23 antibody, in adults with X-linked hypophosphatemia: week 24 primary analysis, J. Bone Miner. Res. 33 (2018) 1383–1393.
[10] H. Li, C.Y. Ji, X.N. Zong, Y.Q. Zhang, Height and weight standardized growth charts for Chinese children and adolescents aged 0 to 18 years, Zhonghua Er Ke Za Zhi 47 (2009) 487–492.
[11] T.D. Thacher, P.R. Fischer, J.M. Pettifor, J.O. Lawson, B.J. Manaster, J.C. Reading, Radiographic scoring method for the assessment of the severity of nutritional rickets, J. Trop. Pediatr. 46 (2000) 132–139.
[12] M.D. Ruppe, X-linked Hypophosphatemia, (2012).
[13] Y. Chi, Z. Zhao, X. He, Y. Sun, Y. Jiang, M. Li, O. Wang, X. Xing, A.Y. Sun, X. Zhou, X. Meng, W. Xia, A compound heterozygous mutation in SLC34A3 causes hereditary hypophosphatemic rickets with hypercalciuria in a Chinese patient, Bone 59 (2014) 114–121.
[14] I.A. Holm, A.E. Nelson, B.G. Robinson, R.S. Mason, D.J. Marsh, C.T. Cowell, T.O. Carpenter, Mutational analysis and genotype-phenotype correlation of the PHEX gene in X-linked hypophosphatemic rickets, J. Clin. Endocrinol. Metab. 86 (2001) 3889–3899.
[15] S. Yu, H. Fang, J. Han, X. Cheng, L. Xia, S. Li, M. Liu, Z. Tao, L. Wang, L. Hou, X. Qin, P. Li, R. Zhang, W. Su, L. Qiu, The high prevalence of hypovitaminosis D in China: a multicenter vitamin D status survey, Medicine (Baltimore) 94 (2015) e585.
[16] C. Oefner, A. D'Arcy, M. Hennig, F.K. Winkler, G.E. Dale, Structure of human neutral endopeptidase (Neprilysin) complexed with phosphoramidon, J. Mol. Biol. 296 (2000) 341–349.
[17] S. Rafaelsen, S. Johansson, H. Raeder, R. Bjerknes, Hereditary hypophosphatemia in Norway: a retrospective population-based study of genotypes, phenotypes, and treatment complications, Eur. J. Endocrinol. 174 (2016) 125–136.
[18] S.S. Beck-Nielsen, K. Brusgaard, L.M. Rasmussen, K. Brixen, B. Brock-Jacobsen, M.R. Poulsen, P. Vestergaard, S.H. Ralston, O.M. Albagha, S. Poulsen, D. Haubek, H. Gjorup, H. Hintze, M.G. Andersen, L. Heickendorff, J. Hjelmborg, J. Gram, Phenotype presentation of hypophosphatemic rickets in adults, Calcif. Tissue Int. 87 (2010) 108–119.
[19] H.Y. Cho, B.H. Lee, J.H. Kang, I.S. Ha, H.I. Cheong, Y. Choi, A clinical and molecular genetic study of hypophosphatemic rickets in children, Pediatr. Res. 58 (2005) 329–333.
[20] M. Zivicnjak, D. Schnabel, H. Billing, H. Staude, G. Filler, U. Querfeld, M. Schumacher, A. Pyper, C. Schroder, J. Bramswig, D. Haffner, Age-related stature and linear body segments in children with X-linked hypophosphatemic rickets, Pediatr. Nephrol. 26 (2011) 223–231.
[21] T.O. Carpenter, K.L. Insogna, J.H. Zhang, B. Ellis, S. Nieman, C. Simpson, E. Olear, C.M. Gundberg, Circulating levels of soluble klotho and FGF23 in X-linked hypophosphatemia: circadian variance, effects of treatment, and relationship to parathyroid status, J. Clin. Endocrinol. Metab. 95 (2010) E352–E357.
[22] K.B. Jonsson, R. Zahradnik, T. Larsson, K.E. White, T. Sugimoto, Y. Imanishi, T. Yamamoto, G. Hampson, H. Koshiyama, O. Ljunggren, K. Oba, I.M. Yang, A. Miyauchi, M.J. Econs, J. Lavigne, H. Juppner, Fibroblast growth factor 23 in oncogenic osteomalacia and X-linked hypophosphatemia, N. Engl. J. Med. 348 (2003) 1656–1663.
[23] D. Sitara, S. Kim, M.S. Razzaque, C. Bergwitz, T. Taguchi, C. Schuler, R.G. Erben, B. Lanske, Genetic evidence of serum phosphate-independent functions of FGF-23 on bone, PLoS Genet. 4 (2008) e1000154.
[24] R. Sapir-Koren, G. Livshits, Bone mineralization is regulated by signaling cross talk between molecular factors of local and systemic origin: the role of fibroblast growth factor 23, Biofactors 40 (2014) 555–568.
[25] M. Morey, L. Castro-Feijoo, J. Barreiro, P. Cabanas, M. Pombo, M. Gil, I. Bernabeu, J.M. Diaz-Grande, L. Rey-Cordo, G. Ariceta, I. Rica, J. Nieto, R. Vilalta, L. Martorell, J. Vila-Cots, F. Aleixandre, A. Fontalba, L. Soriano-Guillen, J.M. Garcia-Sagredo, S. Garcia-Minaur, B. Rodriguez, S. Juaristi, C. Garcia-Pardos, A. Martinez-Peinado, J.M. Millan, A. Medeira, O. Moldovan, A. Fernandez, L. Loidi, Genetic diagnosis of X-linked dominant hypophosphatemic rickets in a cohort study: tubular reabsorption of phosphate and 1,25(OH)2D serum levels are associated with PHEX mutation type, BMC Med. Genet. 12 (2011) 116.
[26] A.J. Turner, R.E. Isaac, D. Coates, The neprilysin (NEP) family of zinc metalloendopeptidases: genomics and function, BioEssays 23 (2001) 261–269.
[27] A.J. Turner, K. Tanzawa, Mammalian membrane metallopeptidases: NEP, ECE, KELL, and PEX, FASEB J. 11 (1997) 355–364.
[28] L. Bianchetti, C. Oudet, O. Poch, M13 endopeptidases: new conserved motifs correlated with structure, and simultaneous phylogenetic occurrence of PHEX and the bony fish, Proteins 47 (2002) 481–488.
[29] P.S. Rowe, C.L. Oudet, F. Francis, C. Sinding, S. Pannetier, M.J. Econs, T.M. Strom, T. Meitinger, M. Garabedian, A. David, M.A. Macher, E. Questiaux, E. Popowska, E. Pronicka, A.P. Read, A. Mokrzycki, F.H. Glorieux, M.K. Drezner, A. Hanauer, H. Lehrach, J.N. Goulding, J.L. O'Riordan, Distribution of mutations in the PEX gene in families with X-linked hypophosphataemic rickets (HYP), Hum. Mol. Genet. 6 (1997) 539–549.
[30] E. Durmaz, M. Zou, R.A. Al-Rijjal, E.Y. Baitei, S. Hammami, I. Bircan, S. Akcurin, B. Meyer, Y. Shi, Novel and de novo PHEX mutations in patients with hypophosphatemic rickets, Bone 52 (2013) 286–291.
[31] F. Francis, T.M. Strom, S. Hennig, A. Boddrich, B. Lorenz, O. Brandau, K.L. Mohnike, M. Cagnoli, C. Steffens, S. Klages, K. Borzym, T. Pohl, C. Oudet, M.J. Econs, P.S. Rowe, R. Reinhardt, T. Meitinger, H. Lehrach, Genomic organization of the human PEX gene mutated in X-linked dominant hypophosphatemic rickets, Genome Res. 7 (1997) 573–585.
[32] C. Gaucher, O. Walrant-Debray, T.M. Nguyen, L. Esterle, M. Garabedian, F. Jehan, PHEX analysis in 118 pedigrees reveals new genetic clues in hypophosphatemic rickets, Hum. Genet. 125 (2009) 401–411.
[33] P.H. Dixon, P.T. Christie, C. Wooding, D. Trump, M. Grieff, I. Holm, J.M. Gertner, J. Schmidtke, B. Shah, N. Shaw, C. Smith, C. Tau, D. Schlessinger, M.P. Whyte, R.V. Thakker, Mutational analysis of PHEX gene in X-linked hypophosphatemia, J. Clin. Endocrinol. Metab. 83 (1998) 3615–3623.
[34] S. Ichikawa, E.A. Traxler, S.A. Estwick, L.R. Curry, M.L. Johnson, A.H. Sorenson, E.A. Imel, M.J. Econs, Mutational survey of the PHEX gene in patients with X-linked hypophosphatemic rickets, Bone 43 (2008) 663–666.
[35] M.D. Ruppe, P.G. Brosnan, K.S. Au, P.X. Tran, B.W. Dominguez, H. Northrup, Mutational analysis of PHEX, FGF23 and DMP1 in a cohort of patients with hypophosphatemic rickets, Clin. Endocrinol. 74 (2011) 312–318.
[36] S. Capelli, V. Donghi, K. Maruca, G. Vezzoli, S. Corbetta, M.L. Brandi, S. Mora, G. Weber, Clinical and molecular heterogeneity in a large series of patients with hypophosphatemic rickets, Bone 79 (2015) 143–149.
[37] S.S. Beck-Nielsen, K. Brixen, J. Gram, K. Brusgaard, Mutational analysis of PHEX, FGF23, DMP1, SLC34A3 and CLCN5 in patients with hypophosphatemic rickets, J. Hum. Genet. 57 (2012) 453–458.
[38] D. Filisetti, G. Ostermann, M. von Bredow, T. Strom, G. Filler, J. Ehrich, S. Pannetier, J.M. Garnier, P. Rowe, F. Francis, A. Julienne, A. Hanauer, M.J. Econs, C. Oudet, Non-random distribution of mutations in the PHEX gene, and under-detected missense mutations at non-conserved residues, Eur. J. Hum. Genet. 7 (1999) 615–619.
[39] S.S. Li, J.M. Gu, W.J. Yu, J.W. He, W.Z. Fu, Z.L. Zhang, Seven novel and six de novo PHEX gene mutations in patients with hypophosphatemic rickets, Int. J. Mol. Med. 38 (2016) 1703–1714.
[40] Y. Sabbagh, G. Boileau, M. Campos, A.K. Carmona, H.S. Tenenhouse, Structure and function of disease-causing missense mutations in the PHEX gene, J. Clin. Endocrinol. Metab. 88 (2003) 2213–2222.
[41] Y. Sabbagh, G. Boileau, L. DesGroseillers, H.S. Tenenhouse, Disease-causing missense mutations in the PHEX gene interfere with membrane targeting of the recombinant protein, Hum. Mol. Genet. 10 (2001) 1539–1546.
[42] C. Weng, J. Chen, L. Sun, Z.W. Zhou, X. Feng, J.H. Sun, L.P. Lu, P. Yu, M. Qi, A de novo mosaic mutation of PHEX in a boy with hypophosphatemic rickets, J. Hum. Genet. 61 (2016) 223–227.
[43] M.P. Whyte, F.W. Schranck, R. Armamento-Villareal, X-linked hypophosphatemia: a search for gender, race, anticipation, or parent of origin effects on disease expression in children, J. Clin. Endocrinol. Metab. 81 (1996) 4075–4080.
[44] D.C. Hardy, W.A. Murphy, B.A. Siegel, I.R. Reid, M.P. Whyte, X-linked hypophosphatemia in adults: prevalence of skeletal radiographic and scintigraphic features, Radiology 171 (1989) 403–414.
[45] E.D. Shields, C.R. Scriver, T. Reade, T.M. Fujiwara, K. Morgan, A. Ciampi, S. Schwartz, X-linked hypophosphatemia: the mutant gene is expressed in teeth as well as in kidney, Am. J. Hum. Genet. 46 (1990) 434–442.
[46] D.J. Petersen, A.M. Boniface, F.W. Schranck, R.C. Rupich, M.P. Whyte, X-linked hypophosphatemic rickets: a study (with literature review) of linear growth response to calcitriol and phosphate therapy, J. Bone Miner. Res. 7 (1992) 583–597.
[47] H.R. Song, J.W. Park, D.Y. Cho, J.H. Yang, H.R. Yoon, S.C. Jung, PHEX gene mutations and genotype-phenotype analysis of Korean patients with hypophosphatemic rickets, J. Korean Med. Sci. 22 (2007) 981–986.